Rashed and Mehanny
Journal of Engineering and Applied Science (2023) 70:28
https://doi.org/10.1186/s44147-023-00199-4

Journal of Engineering and Applied Science

RESEARCH Open Access

Simulating creep induced moment redistribution in prestressed concrete bridges constructed by the balanced cantilever method: ad hoc traditional formulae versus real time-dependent analysis

Magdy Rashed[1*] and Sameh S. F. Mehanny[2]

*Correspondence:
magdy.rashed@dar.com

[1] Dar Al-Handasah, Smart Village, Cairo, Egypt
[2] Cairo University, Cairo, Egypt

Abstract

Assessing available numerical techniques adopted to determine the design time-dependent moment for prestressed concrete segmental bridges constructed by the balanced cantilever method is of utmost importance to the bridge design community. In essence, despite some *apparent* diversity, there are basically two key conventional approaches to compute the design time-dependent moment accounting for creep effects for this type of bridges. The first is a family of varied simplified methods typically known to practicing designers and with pre-consensus on their reliability and effectiveness. Time-dependent moments retrieved from these classical methods always reside in an intermediate state falling between the results from "two" time-*independent* analysis cases, namely, (a) sequentially adding all partial permanent loads and prestressing pertaining to various construction steps using the part-bridge structural system corresponding to each step, and (b) assuming all loads and prestressing forces to be applied at-once to the final completed bridge. The second approach is through performing real sophisticated step-by-step time-dependent analysis using a specialized software. The research primary objective is to assess the validity/reliability of commonly used ad-hoc approaches that evolved over the years relying on simplified analyses/formulae to cater for time-dependent creep effects for this type of bridges. Aiming at realistic conclusions, three case-study real-world segmental balanced cantilever bridges over the Nile River in Egypt are elected. Midas Civil commercial package is used to perform time-dependent finite element analyses for the three bridges. Main parameters considered are, inter alia, time-dependent effects of creep and shrinkage of concrete, relaxation of prestressed steel, losses due to friction and anchor setting of prestressing tendons, sequence of construction, and construction-driven temporary change of support conditions (where applicable). The study concludes that creep-induced moment redistribution from simplified traditional formulae typically adopted in the literature may lead to a considerable error in estimating the design time-dependent moment in balanced cantilever bridges.

Keywords: Segmental bridges, Balanced cantilever, Time-dependent effects, Sequence of construction, Creep

Introduction

Significant progress has been made over the years in the development of step-by-step methodologies to account for the time-dependent effects in the analysis of segmental prestressed concrete bridges. A bunch of diversified articles on the design, analysis, and construction of segmental bridges have been published by many researchers. Prime attention is given to estimating reliable values for the deformations and internal moment redistribution due to creep and shrinkage of concrete as the structural system is changing during successive construction phases [1–14]. In particular, Bishara and Papakonstantinou [11] investigated the time-dependent deformation of cantilever construction bridges before and after closure. Cruz et al. [15] introduced a nonlinear analysis method to calculate the ultimate strength of bridges. Simplified formulae for estimating the internal moment redistribution due to creep and shrinkage of concrete have been always eagerly awaited by the bridge design community. Trost and Wolff [14] proposed an intuitive formula (namely, Eq. 1) that started since then to gain worldwide reputation and acceptance. It is based on combining elastic moments, $\Sigma M_{s,i}$, that occur at successive construction steps (see Fig. 1) on the one hand, and the moment obtained by assuming the entire structure constructed at one same stage, M_E, at the other hand:

$$M_T = \sum M_{s,i} + (M_E - \sum M_{s,i}) \frac{\varnothing_t}{1 + \rho \varnothing_t} \tag{1}$$

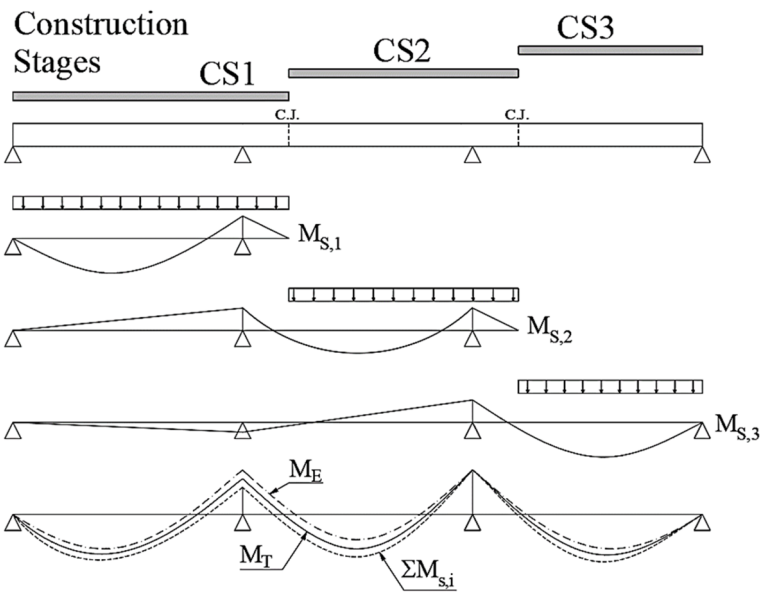

Fig. 1 Schematic showing combination of elastic moments for segmental bridges using span-by-span construction techniques. M_T estimated time-dependent moment. M_E moment obtained by assuming the entire structure constructed at one same stage. ΣMs,i combination of elastic moments occurring at each construction stage after scaffolding removal

where ϕ_t and ρ represent the creep and corresponding relaxation factors, respectively. A similar approach has been presented by the Prestressed Concrete Institute and Post-Tensioning Institute [16]. Furthermore, Kwak and Son [17], yet adopting the same format traditionally introduced in the literature to combine pre-elected elastic moments from different statical systems of the bridge under consideration, namely Eq. (1), proposed a slight alteration as reflected in Eq. (2), in order to determine the design moments in bridges constructed by the balanced cantilever method to account for time-dependent creep effects. They claim that there should be some limitations if applying Eq. (1) to balanced cantilever bridges since the creep-induced moments grow continuously from each time the structural system changes throughout consecutive construction steps (t = c days). Maintaining the basic form of Eq. (1) suggested by Trost and Wolff [14], yet considering the actual construction sequence while calculating the internal moments at an arbitrary time t, Kwak and Son [17] proposed another *simplified* ad hoc equation as follows:

$$M_T = \sum M_{s,i} + \left(M_E - \sum M_{s,i}\right)\left(1 - e^{-(\varnothing_t - \varnothing_c)}\right) f(\varnothing_t) \tag{2}$$

where $f(\phi_t) = \chi\phi_t/(1+\chi\phi_t)$. χ is the concrete ageing coefficient [18–22] which accounts for the effect of ageing on the ultimate value of creep for stress increments or decrements occurring gradually after application of the original load. As explicitly revealed in Kwak and Son [17], the following primary differences can be sorted out when comparing Eq. (2) with Eq. (1): (*i*) to simulate the cantilevered construction, the term $(1 - e^{-(\phi t - \phi c)})$ describing the creep behavior of a cantilevered beam has been included in Eq. (2); and (*ii*) the term $\phi_t/(1+\rho\phi_t)$ in Eq. (1) is replaced by the functional $f(\phi_t) = \chi\phi_t/(1+\chi\phi_t)$ in Eq. (2) on the basis of the relaxation phenomenon.

Recently, following in previous researchers' footsteps, Gendy and Rashed [23] adopted similar format of formerly established simplified formulae but introduced some optimization-derived combination factors. Time-dependent moments along the bridge length are still extracted from 'two' conventional time-*independent* analysis models. The first consists of a family of models representing the construction sequence, and a combined moment, ΣM_O, is then computed by superposing all partial moments, M_{Oj}, obtained from various successive construction steps using the statical system corresponding to each step ignoring time-dependent effects. The second model then assumes all relevant loads and prestressing forces to be applied to the final structural system of the completed bridge after installing the closure segment, and the corresponding 'one-go' moment, M_C, is hence calculated. The final time-*dependent* moment, $M_{T,est.}$, can be thus estimated from *linearly* combining the two contributions of this couple of time-*independent* (and simultaneously conducted) analyses as per Eq. (3):

$$M_{T,est.} = \alpha \sum M_{O_j} + \beta M_C \tag{3}$$

where α and β are pre-assumed combination parameters purposely concocted to approximately simulate the time-dependent effects. These linear combination coefficients α and β are always classically constrained to a unit sum, thus combining the two time-*independent* moment terms in a manner similar to antecedent traditional formulae as illustrated by Eqs. (1) and (2). An optimization algorithm has been introduced by Gendy

and Rashed [23] to cast the estimation of these parameters considering real-world two balanced cantilever prestressed concrete bridges. α and β are found sensitive to the time schedule of construction, and accordingly some recommended values for these parameters are given for different construction scenarios.

It has to be noted that the format traditionally adopted when *linearly* combining the two time-*independent* moment terms–featuring either (*i*) some implicit combination coefficients that add up to a unity (viz. Eqs. (1) and (2)), or (*ii*) explicit combination coefficients with a unit sum such as α and β of Eq. (3)—results in final design time-*dependent* creep-accounting moment "always" bounded by the values of the moments retrieved from the two time-*independent* analyses illustrated above. Such anticipated trend as pre-dictated by the classical *linear* combination format with "unit sum constrained" combination coefficients has been refuted by Pimanmas [24] for a real-world case study prestressed concrete segmental bridge in Thailand constructed by the balanced cantilever method. Contradicting general consensus among designers, the results presented in Pimanmas [24] show that the creep can increase the magnitude of hogging moment, rather than decreasing it as widely anticipated. As further illustrated by the author, this is usually the case if the prestressing amount in the top cables exceeds circa 70% of the ultimate tensile strength of the cables and is, as such, beyond a certain appreciable threshold value relative to the bridge dead weight effects. Accordingly, all simplified formulae (adopting the supposedly intuitive 'constrained *linear* combination' format) commonly known to practicing designers to estimate the long-term creep-induced moment as a fraction of (a) sequentially retrieved and superimposed dead load and prestressing moments from successive construction stages up to completion, and (b) moment in the continuous state from one-go time-independent analysis of the complete bridge, have been rebutted for balanced cantilever construction.

It is finally worth highlighting that simplified methods for determining time-dependent moment redistribution in segmental prestressed concrete bridges through ad-hoc formulae combining results from different statical systems (viz. a series of 'open' bridge successive configurations literally following consecutive construction steps; and a 'closed', i.e., completed bridge) using some reasonably pre-selected/optimized weighting factors has emanated in the early literature for *span-by-span* construction using movable scaffolding systems (Schlaich and Scheef [25], and Trost and Wolff [14], among others). Tweaking this simplified approach by numerous researchers and designers through fine tuning the 'unit sum-constrained' combination coefficients to suit segmental prestressed concrete bridges constructed by the *balanced cantilever* method might be a bold extrapolation. Such step would have needed further careful investigations prior to considering the technique as sound and reliable, and hence holding the approach as the design method of choice in absence of specialized software able to conduct sophisticated step-by-step time-dependent analysis accounting for creep effects. As a long-awaited effort, and building upon earlier work by Pimanmas [24], the current research contributes towards assessing the robustness and validity of such simplified 'linear combination' formulae to determine design time-depended moments in real-world *balanced cantilever* prestressed concrete bridges.

Methods

The research primary aim is to assess the validity of typically adopted ad-hoc approaches that evolved over the years relying on simplified analyses and formulae to cater for time-dependent creep effects for this type of bridges. Targeting realistic conclusions, three case-study actual segmental balanced cantilever bridges over the Nile River in Egypt (namely, El Warrak, Girga and Talkha bridges) are considered. Midas Civil commercial package is used to perform time-dependent finite element analyses for the three bridges. Main parameters considered are, inter alia, time-dependent effects of creep and shrinkage of concrete, relaxation of prestressed steel, losses due to friction and anchor setting of prestressing tendons, sequence of construction, and construction-driven temporary change of support conditions (where applicable).

Application to segmental prestressed concrete bridges constructed by the balanced cantilever method

Three case studies of real-world segmental prestressed concrete bridges over the Nile River in Egypt, namely, El-Warrak Bridge, Girga Bridge and Talkha Bridge constructed by the balanced cantilever method are considered herein. El-Warrak Bridge is located in Cairo Governorate, the capital of Egypt and constructed in 2001; Girga Bridge is located in Sohag Governorate in upper Egypt and constructed in 2012; and Talkha Bridge is located in Dakahlia governorate in the Nile delta area to the north of Cairo and constructed in 2011. The key target is to accurately determine the time-dependent bending moments along these bridges accounting for all relevant long-term factors. Midas Civil commercial software is first used to perform a sophisticated time-dependent finite element analysis for the three bridges. The actual construction schedule of each bridge available to the authors has been followed while performing the construction stages analysis. Eurocode models [26] for creep, shrinkage, compressive strength, relaxation of prestressed steel, and losses in prestressing tendons have been utilized for the time-dependent analysis. In a complementary step and for comparison purposes, the simplified approach in Kwak and Son [17] has been adopted to determine some estimates for the time-dependent moments along each of the case study bridges considering all relevant actual parameters, namely, properties of cross-sections, ambient relative humidity, age at loading of each segment, time of closure of the structural system, etc. The main objective of the study is to critically compare results obtained from the simplified (i.e., combination formula-driven time-*independent*) versus sophisticated (viz. real time-*dependent*) analysis approaches, and accordingly assess the suitability of applying simplified approaches to this type of bridges constructed by the balanced cantilever method.

Case study Bridge 1: El-Warrak Bridge

Bridge description

El-Warrak Bridge is among the longest segmental prestressed balanced cantilever bridges over the Nile River in Egypt. The bridge has a total length of 380 m, with a maximum span length of 120 m (Fig. 2). The bridge consists of four spans, two 120 m navigational (center) spans and two 70 m side spans. It has eight lanes, i.e., four lanes for each traffic direction. The cross-section of the bridge consists of a four-cell hunched box girder;

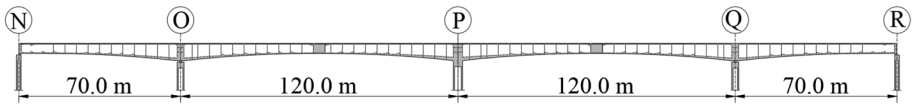

Fig. 2 Elevation of El-Warrak Bridge over the Nile River

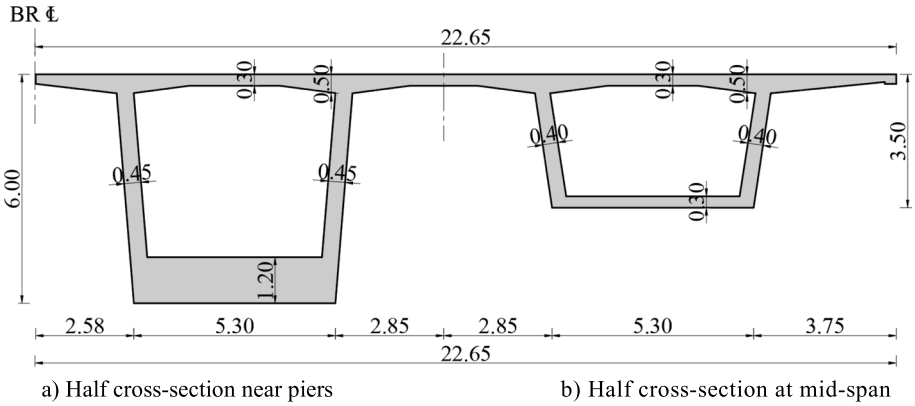

Fig. 3 Typical cross-sections of El-Warrak Bridge. **a** Half cross-section near piers. **b** Half cross-section at mid-span

each direction has a double-cell box girder completely separated in the longitudinal direction of the bridge. The double-cell box has slanted webs and two side cantilevers providing a roadway of 22.65 m wide, as shown in Fig. 3. The girder depth varies over the length following second-degree parabola from the maximum of 6.0 m over the piers to a minimum of 3.5 m at the middle of the main spans. The thickness of the bottom slab varies also parabolically from a maximum of 1.20 m at the piers to a minimum of 0.30 m at the middle of the main span. The bridge is built using the cantilever method. Three double cantilever parts are constructed independently, i.e., around the O, P, and Q axes. Each double cantilever is constructed in segments starting from the pier towards the center spans, i.e., one segment from the right end followed by another one from the left end, etc. Each segment is 5.0 m long except for three segments of length 2.5 m (i.e., one near each of piers O, P, and Q) to maintain/limit the unbalanced length between the two arms of the cantilevers during construction equal to 2.5 m. Two travelers, one at each tip of the two cantilevers, are utilized to erect segments. After the erection of each segment, it is post-tensioned to the previous segment (i.e., the one located on the other end of the double cantilever) with "cantilever" tendons located in the top slab of the cross-section referred to as top prestressing cables. After closure at all transition piers (viz. piers at axes N & R) and at mid-span, the entire bridge is prestressed with several additional "continuity" tendons in zones with high sagging (i.e., positive) moments. The longitudinal prestressing layout is shown in Fig. 4, each tendon consists of 12, 0.6-inch (15.7 mm) diameter strands and is stressed from one end.

Actual construction sequence

The bridge is incrementally constructed as a balanced cantilever from piers O, P, and Q, as schematically depicted in Table 1. A set of 21 cast-in-place segments are installed sequentially at both sides of each of the two piers O and Q, while 22 segments are

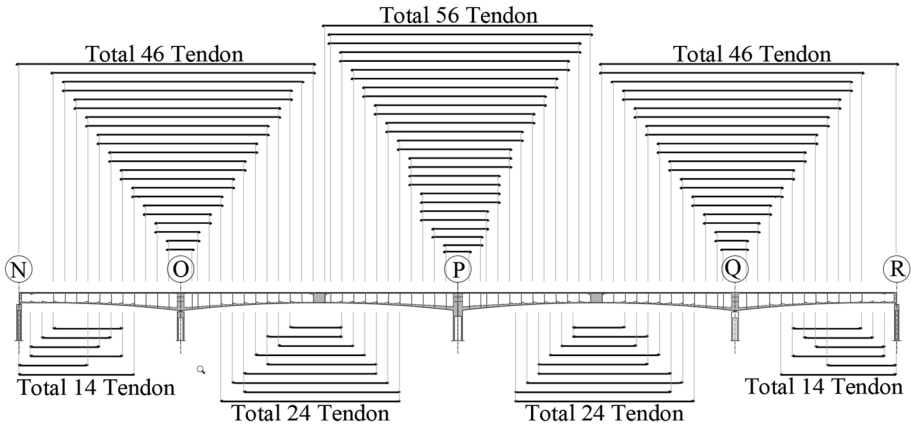

Fig. 4 Longitudinal prestressing layout of El-Warrak Bridge ("cantilever" and "continuity" tendons)

Table 1 Actual construction sequence of El-Warrak Bridge

Stage #	Duration (day)	Description
1	90	- Substructure casting (piles, pile-caps, and piers)
2	30	- Pier table casting at piers "O", "P", and "Q" - Stressing of the associated cantilever tendons
3 to 23	147 (21 stage × 7 days)	- Casting of full-cantilevers segments at piers "O", "P", and "Q" (20 segments around each of the two piers O and Q) - Casting 21 segments around pier P - Stressing of the cantilever tendons associated with the cast segments in these stages
24	30	- Completion of the cantilever segments around pier "P" (22 segments) - Casting the off-shore segments in the side spans (near piers "N" and "R") - Stressing of the associated cantilever tendons. In addition, stressing 8 bottom "continuity" tendons in each side span
25	14	- Casting of closure segments - Stressing 6 bottom "continuity" tendons in each main span
26	7	- Stressing the remaining bottom "continuity" tendons in main spans and side spans
27	7	- Replacement of the temporarily fixed connections at piers "O" and "Q" by sliding pot bearings in the longitudinal direction of the bridge

constructed around axis P. During construction, piers O and Q are temporarily fixed to the superstructure by means of vertical prestressing to avoid instability produced by unbalanced cantilever moment. Each segment is cast utilizing conventional formwork in 7 days, while the construction of each pier takes 90 days in addition to 30 days for the stump (i.e., pier table segments). On the two sides of the river, a 15.0-m-long portion

located at one end of each side span is cast on temporary scaffolding and then connected to the segmentally erected double cantilevers located at axes O and Q. After the side span hardens, 8 bottom tendons are locally tensioned in each side span. The tips of the cantilevers in the navigation spans are then connected by 5.0-m-long closure segments. After the two closure segments harden, 24 bottom tendons are prestressed in each navigation span along with 6 more bottom tendons in each side span. The construction of the entire bridge takes 311 days. After all bottom continuity tendons are prestressed, the structure achieves its 'final' continuous form. Any load applied afterwards, namely, superimposed load including asphaltic wearing surface and safety barriers, traffic loads and other live loads will act on the closed bridge having a *continuous* structural system.

Finite element analysis of the bridge structure

A finite element analysis is conducted using Midas Civil (2021) commercial software. Figure 5 shows the three-dimensional model of the bridge built to simulate the behavior during construction and throughout the bridge full service life accounting for the long-term time-dependent creep effects. Numerical analysis is performed adopting a step-by-step strategy for segmental prestressed concrete bridges, considering each increase in the applied loads introduced by successively erecting each new segment and tensioning new tendons. The actual construction sequence of the bridge has been respected in the construction-stage analysis of the FE model. Eurocode specifications as per *EN 1992-1-1(2004)* and *EN 1992-2 (2005)* [26, 27], as well as CEB-FIB [28] and AASHTO LRFD [29] provisions/models for comparison purposes, have been utilized to account for all relevant parameters that affect the time-dependent analysis such as creep, shrinkage, compressive concrete strength, and losses of prestressing tendons.

Results and discussion

Sophisticated real step-by-step time-dependent FE analysis

The design time-dependent moment at any section along the bridge length is captured by a 3D time-history step-by-step FE analysis literally following the construction sequence in Table 1. Final moments are obtained from the summation of the bending moments due to all permanent loads such as the self-weight of the bridge deck, the primary moment of prestressing steel and the secondary (i.e., parasitic/indeterminate) moment

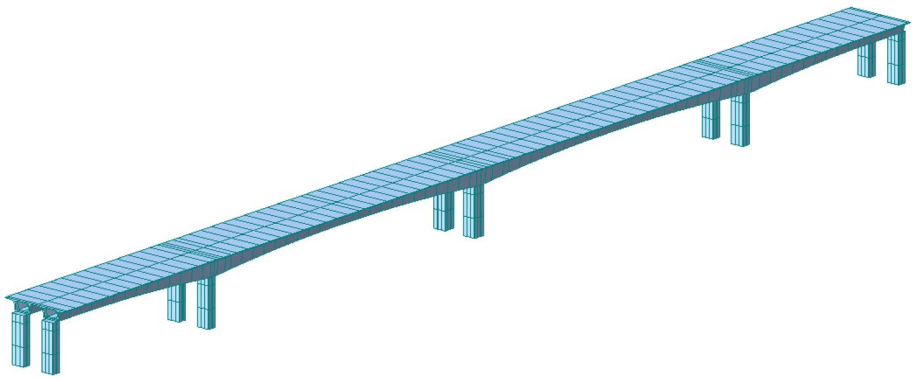

Fig. 5 3D FE model of El-Warrak Bridge in Midas Civil software

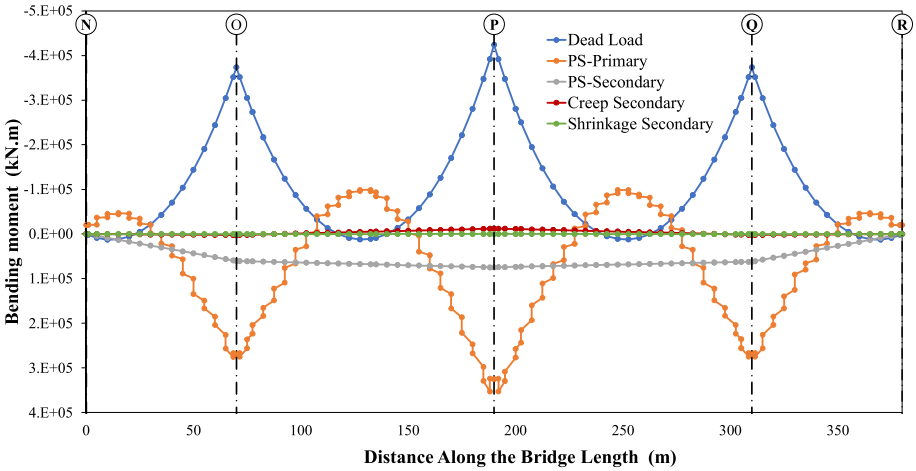

Fig. 6 Itemized bending moments along El Warrak Bridge length from various permanent loads at age of 10,000 days

caused by the prestressing action, as well as the long-term effects due to creep and shrinkage of concrete and losses in the prestressing steel. For illustration purposes, Fig. 6 shows a break-down of the bending moments for all applicable loads after 10,000 days. This duration has been assumed to appropriately capture and scrutinize the long-term effects. The 'full' (viz. *combined*) design time-dependent moment (viz. summation of all itemized components depicted in Fig. 6) is provided in Fig. 8.

Simplified method per available linear combination formula by Kwak and Son (2002) [17]

The simplified Eq. (2) introduced by Kwak and Son [17] is used to find some estimate for the design time-*dependent* moment along the bridge length. The bending moment values in the two combined terms of Eq. (2) refer to the results obtained from two conventional time-*independent* analysis models as described above. The first series/family of models follow the actual construction sequence considering the structure's statical system at each construction stage and then superposing all partial moments retrieved from successive steps/phases in order to compute $\Sigma M_{s,i}$. The second model assumes that all relevant loads and prestressing forces are applied in *one-go* to the final statical system of the complete, i.e., 'continuous', bridge to calculate the moment, M_E. These time-*independent* FE analyses have been also conducted using Midas Civil software package to estimate reasonable values of the time-*independent* moments ($\Sigma M_{s,i}$ and M_E) referred to in Eq. (2). In addition, relevant creep factors for each segment along the bridge length have been calculated: namely, ϕ_c, at the time at which the closure segment is installed, i.e., just after closing the bridge deck ($t = c$ days) to achieve a continuous structural system; and ϕ_t, at the time considered herein to capture and inspect the long-term effects (i.e., $t = 10{,}000$ days). On the other hand, the functional $f(\phi_t) = \chi\phi_t/(1+\chi\phi_t)$ in Eq. (2), as addressed in Kwak and Son [17], assumes values of 0.62, 0.64, and 0.65 at 1, 10, and 100 years, respectively [17–19, 22]. A value of 0.645 for $f(\phi_t)$ has been adopted herein corresponding to 10,000 days. For completeness, Table 2 illustrates the calculation of creep factors for all segments along the bridge length. Finally, Fig. 7 provides the estimated design time-*dependent* moment, M_T, along the bridge length according to

Table 2 Creep factors calculation according to EN 1992-1-1:2004 for El-Warrak Bridge segments (please refer to EN 1992-1-1 for notations and definitions)

Segment #	t_o (day)	t_1 (day)	t_2 (day)	h_o (mm)	φ_{RH}	$\beta(t_0)$	φ_0	β_H	$\beta_c(t_2-t_0)$	$\beta_c(t_1-t_0)$	$\Delta\beta_c(t_2-t_1)$	$\varphi(t_2,t_1)$ $(\varphi_t-\varphi_c)$
1	7	207	10,000	440	1.335	0.635	2.054	875.3	0.975	0.614	0.361	0.742
2	7	207	10,000	440	1.335	0.635	2.054	875.3	0.975	0.614	0.361	0.742
3	7	207	10,000	440	1.335	0.635	2.054	875.3	0.975	0.614	0.361	0.742
4	7	207	10,000	450	1.332	0.635	2.049	890.3	0.975	0.611	0.364	0.745
5	7	170	10,000	460	1.329	0.635	2.045	905.3	0.974	0.609	0.366	0.747
6	7	156	10,000	480	1.323	0.635	2.036	935.4	0.974	0.604	0.370	0.753
7	7	142	10,000	490	1.321	0.635	2.032	950.5	0.973	0.602	0.372	0.755
8	7	128	10,000	510	1.316	0.635	2.024	980.5	0.972	0.597	0.375	0.760
9	7	114	10,000	520	1.313	0.635	2.021	995.6	0.972	0.595	0.377	0.762
10	7	100	10,000	540	1.308	0.635	2.013	1025.7	0.971	0.590	0.381	0.767
11	7	86	10,000	550	1.306	0.635	2.010	1040.7	0.971	0.588	0.382	0.769
12	7	72	10,000	570	1.302	0.635	2.003	1070.8	0.970	0.584	0.386	0.773
13	7	58	10,000	580	1.300	0.635	2.000	1085.8	0.970	0.582	0.387	0.775
14	7	44	10,000	590	1.298	0.635	1.997	1100.9	0.969	0.580	0.389	0.777
15	7	30	10,000	610	1.294	0.635	1.991	1131.0	0.968	0.576	0.392	0.781
16	7	30	10,000	1750	1.189	0.635	1.829	1280.9	0.964	0.558	0.406	0.743
17	7	30	10,000	1750	1.189	0.635	1.829	1280.9	0.964	0.558	0.406	0.743
18	7	30	10,000	610	1.294	0.635	1.991	1131.0	0.968	0.576	0.392	0.781
19	7	37	10,000	600	1.296	0.635	1.994	1115.9	0.969	0.578	0.391	0.779
20	7	51	10,000	590	1.298	0.635	1.997	1100.9	0.969	0.580	0.389	0.777
21	7	65	10,000	570	1.302	0.635	2.003	1070.8	0.970	0.584	0.386	0.773
22	7	79	10,000	560	1.304	0.635	2.007	1055.7	0.970	0.586	0.384	0.771
23	7	93	10,000	540	1.308	0.635	2.013	1025.7	0.971	0.590	0.381	0.767
24	7	107	10,000	530	1.311	0.635	2.017	1010.6	0.972	0.593	0.379	0.764
25	7	121	10,000	510	1.316	0.635	2.024	980.5	0.972	0.597	0.375	0.760
26	7	135	10,000	500	1.318	0.635	2.028	965.5	0.973	0.599	0.373	0.757

Table 2 (continued)

Segment #	t_o (day)	t_1 (day)	t_2 (day)	h_o (mm)	φ_{RH}	$\beta(t_0)$	φ_0	β_H	$\beta_c(t_2\text{-}t_0)$	$\beta_c(t_1\text{-}t_0)$	$\Delta\beta_c(t_2\text{-}t_1)$	$\varphi(t_2,t_1)$ (φ_t-φ_c)
27	7	149	10,000	480	1.323	0.635	2.036	935.4	0.974	0.604	0.370	0.753
28	7	163	10,000	460	1.329	0.635	2.045	905.3	0.974	0.609	0.366	0.747
29	7	170	10,000	450	1.332	0.635	2.049	890.3	0.975	0.611	0.364	0.745
30	7	221	10,000	440	1.335	0.635	2.054	875.3	0.975	0.614	0.361	0.742
31	7	207	10,000	450	1.332	0.635	2.049	890.3	0.975	0.611	0.364	0.745
32	7	170	10,000	460	1.329	0.635	2.045	905.3	0.974	0.609	0.366	0.747
33	7	156	10,000	490	1.321	0.635	2.032	950.5	0.973	0.602	0.372	0.755
34	7	142	10,000	510	1.316	0.635	2.024	980.5	0.972	0.597	0.375	0.760
35	7	128	10,000	530	1.311	0.635	2.017	1010.6	0.972	0.593	0.379	0.764
36	7	114	10,000	550	1.306	0.635	2.010	1040.7	0.971	0.588	0.382	0.769
37	7	100	10,000	580	1.300	0.635	2.000	1085.8	0.970	0.582	0.387	0.775
38	7	86	10,000	600	1.296	0.635	1.994	1115.9	0.969	0.578	0.391	0.779
39	7	72	10,000	620	1.292	0.635	1.988	1146.0	0.968	0.574	0.394	0.783
40	7	58	10,000	640	1.288	0.635	1.982	1176.1	0.967	0.570	0.397	0.786
41	7	44	10,000	660	1.285	0.635	1.977	1206.2	0.966	0.567	0.400	0.790
42	7	30	10,000	670	1.283	0.635	1.974	1221.2	0.966	0.565	0.401	0.792
43	7	30	10,000	1750	1.189	0.635	1.829	1280.9	0.964	0.558	0.406	0.743

The bridge contains 80 segments; the numbering of segments is in an ascending order from segment #1 at pier N to segment #86 at pier R. The above table contains the segments in the half-length of the bridge

t_o age of segment at loading, t_1 age at segment placement; $t_2 = 10{,}000$ days (long-term)

h_o Notional size of the member (segment)

φ_o Notional creep coefficient

φ_{RH} Factor to allow for the effect of relative humidity on the notional creep coefficient

$\beta(t_o)$ Factor to allow for the effect of concrete age at loading on the notional creep coefficient

β_H Coefficient depending on the relative humidity

$\beta c(t,t_0)$ Coefficient to describe the development of creep with time after loading

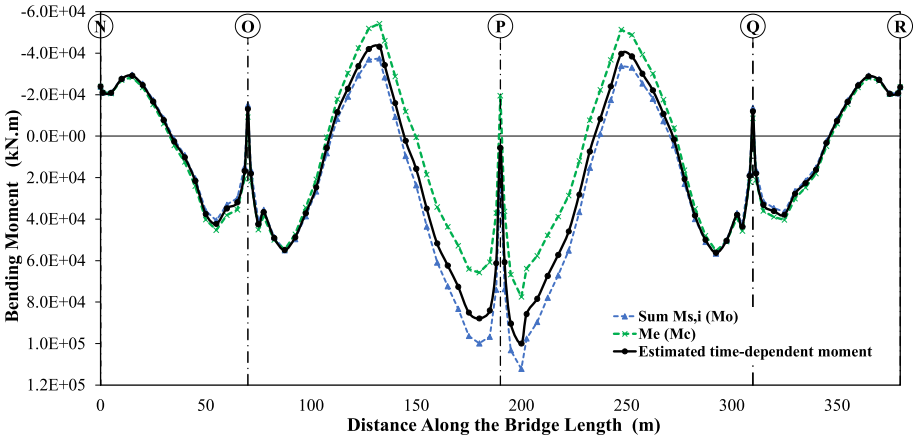

Fig. 7 Estimated time-dependent moments using the simplified approach per Kwak and Son (2002)–El Warrak Bridge

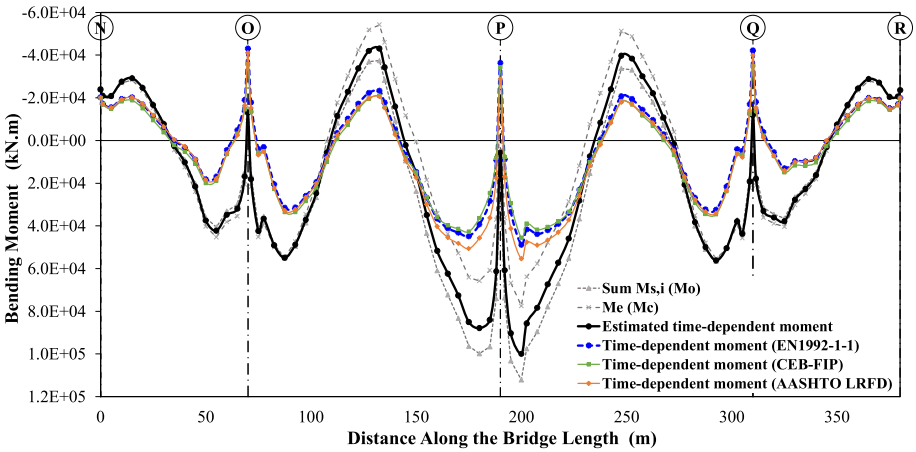

Fig. 8 Time-dependent moments from 'real' time history FE analysis versus estimated time-dependent moment from simplified approach–El Warrak Bridge

the simplified formula in Eq. (2), as well as its combinatory constituents (namely, $\Sigma M_{s,i}$ and M_E) resulting from the two conventional time-independent FE analyses. It is worth highlighting that as mathematically anticipated by the linear combination format of Eq. (2) with implicit combination coefficients summing up to 1.0, M_T values along the whole bridge length are always bounded by the two combined terms $\Sigma M_{s,i}$ and M_E.

Comparative assessment of results

The main purpose of this section is to compare the results of the time-dependent moments obtained from (*i*) sophisticated real step-by-step time-*dependent* FE analysis versus (*ii*) simplified formula (viz. Eq. (2)) combining results from conventional time-*independent* FE analyses. Figure 8 shows the design time-dependent bending moments along the bridge length for the two approaches.

Results reveal, unexpectedly to the design community, a significant difference between the two approaches. In the two-balanced cantilever construction, as the amount of top

prestressing increases for a particular bridge configuration, the magnitude of creep redistribution is highly likely to get reduced. This may be explained by the fact that this top (i.e., cantilever) prestressing introduced during the open-bridge construction stages acts opposite to the bridge deck own weight and hence restricts creep movement produced by sustained self-weight stresses in the closed bridge structural system. Further increase in top prestressing amount could nullify creep induced by self-weight and may even reverse the creep redistribution since it moves up the cantilever tip against gravity. Accordingly, the prestressing-induced creep increases the design hogging (i.e., over support) moment magnitude (irrespective of the creep model used) in contradiction with traditional simplified formulae as shown in Fig. 8. For further demonstration, the moment due to creep along the prestressed bridge deck has been isolated and presented in Fig. 9 for various construction stages from the time of installation of the closure segment up to 10,000 days in order to display development of creep effects with time. The trend of results in figure seems to contradict widely anticipated time-dependent creep effects in typical segmentally constructed RC bridges or in archetypal prestressed concrete bridges constructed by the span-by-span erection methods. For completeness, a separate time-dependent FE analysis is conducted but excluding prestressing in order to obtain the creep moment distribution along the bridge length due to the sustained self-weight stresses only such as for typical segmentally constructed RC bridges, and results are shown in Fig. 10. When comparing trends in Figs. 9 and 10, it is obvious that the top prestressing in balanced cantilever construction is responsible for limiting self-weight induced creep in the closed bridge configuration, and that some amount of such 'cantilever' prestressing beyond a given threshold could even reverse the bending moment redistribution trend along the bridge deck length due to creep.

On the other hand, the sagging (or *loosely speaking* 'all within-span') moments are appreciably reduced relative to those estimated through the *linear* combination simplified formulae available in the literature as also revealed in Fig. 8. Another important note is that the final design moment including creep due to self-weight and prestressing long-term effects lies outside the range of values bounded by the two (referring to light

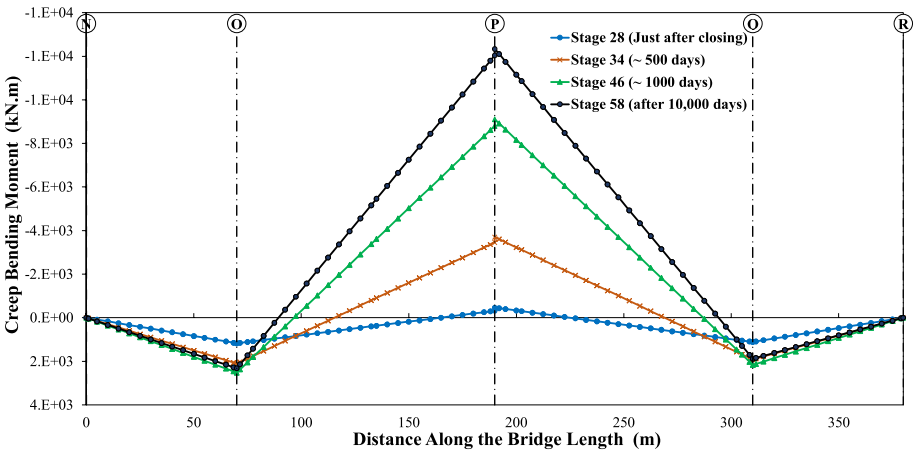

Fig. 9 Creep-induced bending moment due to all permanent loads along El-Warrak prestressed bridge deck at different ages starting from end of construction (i.e., after installing closure segments and applying all continuity prestressing)

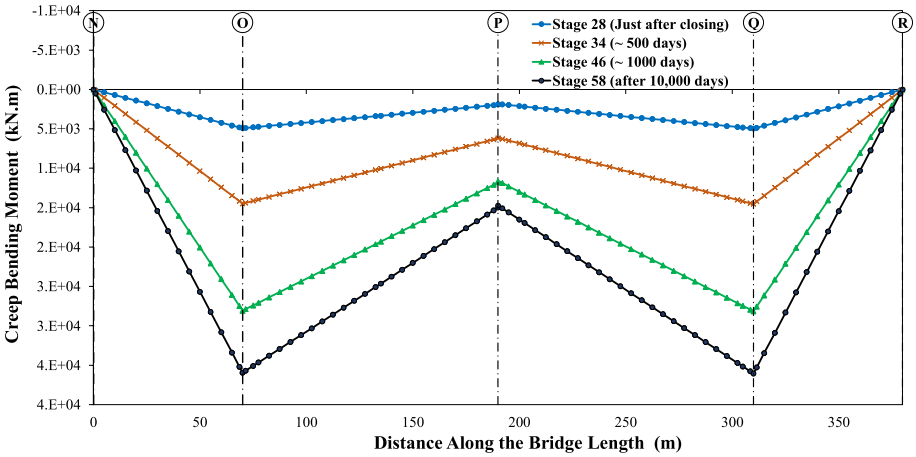

Fig. 10 Self-weight creep-induced bending moment along El-Warrak Bridge deck excluding prestressing effects for illustration purposes

grey curves in Fig. 8) time-*independent* moment terms of the simplified formula, namely Eq. (2), at all cross-sections along the whole length of the bridge.

Case study bridge 2: Girga Bridge

Girga Bridge is one of the longest segmental prestressed balanced cantilever bridges over the Nile River in Egypt. The bridge is 410 m in length, with a maximum span of 130 m (Fig. 11). The bridge consists of four spans, two 130 m navigational (center) spans and two 75 m side spans. It has four lanes, i.e., two lanes for each traffic direction. The superstructure consists of two parallel identical box girders which are completely separated along the longitudinal direction of the bridge. The cross-section of the box girder has vertical webs and two side cantilevers providing a roadway of

Fig. 11 Elevation of Girga Bridge over the Nile River

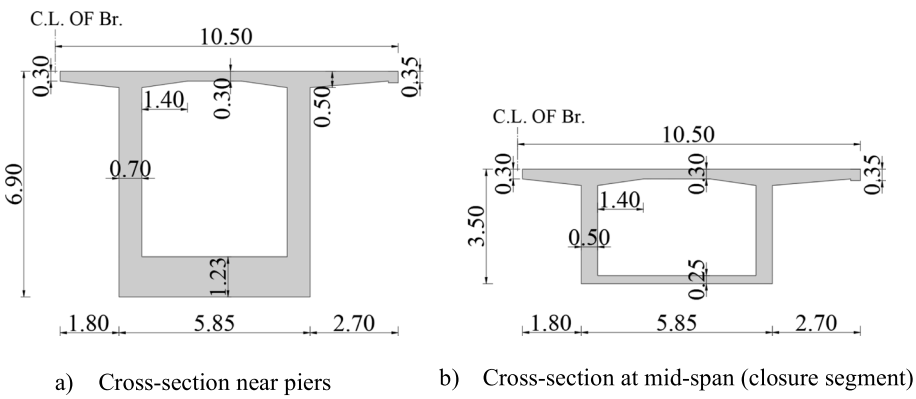

a) Cross-section near piers b) Cross-section at mid-span (closure segment)

Fig. 12 Typical cross-sections of Girga Bridge. **a** Cross-section near piers. **b** Cross-section at mid-span (closure segment)

10.5 m wide, as shown in Fig. 12. The girder depth varies over the length following second-degree parabola with a maximum depth of 6.9 m over the piers to a minimum depth of 3.5 m at the middle of the main spans. The thickness of the bottom slab varies also parabolically from a maximum of 1.23 m at the piers to a minimum of 0.25 m at the middle of the main spans. The bridge is built using the cantilever method. Three double cantilever parts are constructed independently, i.e., around the N13, N14, and N15 axes. Each double cantilever is constructed in segments starting from the pier towards the center spans, i.e., one segment from the right end followed by another one from the left end, etc. Two travelers, one at each tip of the two cantilevers, are utilized to erect segments. After the erection of each segment, it is post-tensioned to the previous segment (i.e., on the other end of the double cantilever) with "cantilever" tendons located in the top slab of the cross-section referred to as top prestressing cables. After closure at all transition piers (viz. piers at axes N12 & N16) and at mid-span, the entire bridge is prestressed with several additional "continuity" tendons in zones with high sagging (i.e., positive) moments. The longitudinal prestressing layout is shown in Fig. 13, each tendon consists of 12, 0.6-inch (15.7 mm) diameter strands and is stressed from one end.

Actual construction sequence

The bridge is incrementally constructed as a balanced cantilever from piers N13, N14, and N15. A set of 23 cast-in-place segments are installed sequentially at both sides of each pier. The bridge is supported on sliding bearings at edge piers (namely, N12 and N16) while it is cast integrally (i.e., monolithically) with intermediate piers (viz. N13, N14, and N15). Each segment is cast utilizing conventional formwork in 7 days, while the construction of piers takes 90 days in addition to 30 days for the stump (i.e., pier table segment). On the two sides of the river, a 12.5-m-long portion located at one end of each side span is cast on temporary scaffolding and then connected to the segmentally erected double cantilevers located at axes N13 and N15. After the side span hardens, 6 bottom tendons are locally tensioned in each side span. The tips of the cantilevers in the navigation spans are then connected by 5.0-m-long closure segments. After the two closure segments harden, 26 bottom tendons are prestressed in each navigation span along with 10 more bottom tendons in each side span. The construction of the entire bridge takes 325 days. After all bottom continuity

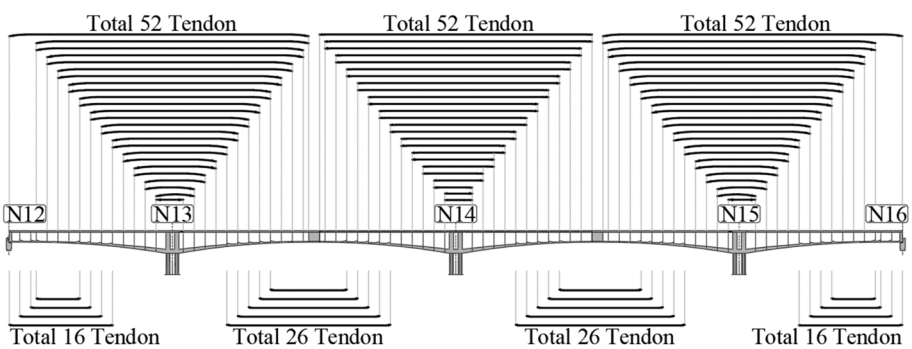

Fig. 13 Longitudinal prestressing layout of Girga Bridge

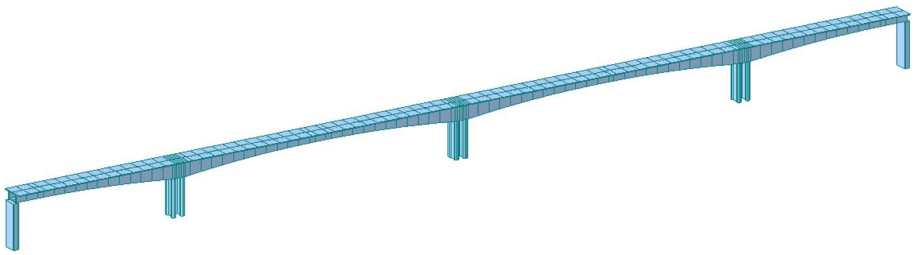

Fig. 14 3D FE model of Girga Bridge in Civil Midas software

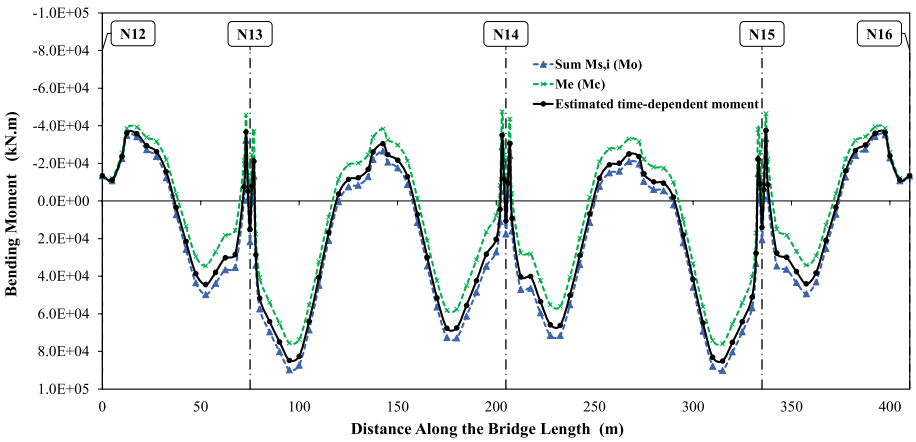

Fig. 15 Estimated time-dependent moments along Girga Bridge using the simplified approach per Kwak and Son (2002)

tendons are prestressed, the structure achieves its 'final' continuous/complete form Fig. 14 shows the three-dimensional model of the bridge built to simulate the behavior during construction and throughout the bridge full service life accounting for the long-term time-dependent creep effects.

Results of the two analysis approaches and comparative assessment of results

Same analysis schemes adopted for El-Warrak Bridge have been also followed for Girga Bridge. In addition, relevant creep factors (ϕ_c and ϕ_t) for each segment along the bridge length have been calculated according to EN 1992-1-1:2004 [26] but not included herein for space limitations; refer to Rashed [30] for a set of complete data. Figure 15 provides the estimated design time-dependent moments along the bridge length according to the simplified formula in Eq. (2), as well as its constituents (namely, ΣMs,i and M_E) resulting from the two conventional time-*independent* FE analyses as demonstrated before. On the other hand, the second approach (actual time-dependent analysis) is adopted by performing a sophisticated time history FE analysis using Midas Civil considering the actual construction sequence of the bridge as well as all relevant parameters that affect the time-dependent analysis. The time-dependent moments along the bridge after 10,000 days are accordingly obtained.

Finally, Fig. 16 illustrates the design time-dependent bending moments along the bridge length according to the two approaches for comparative purposes. Results

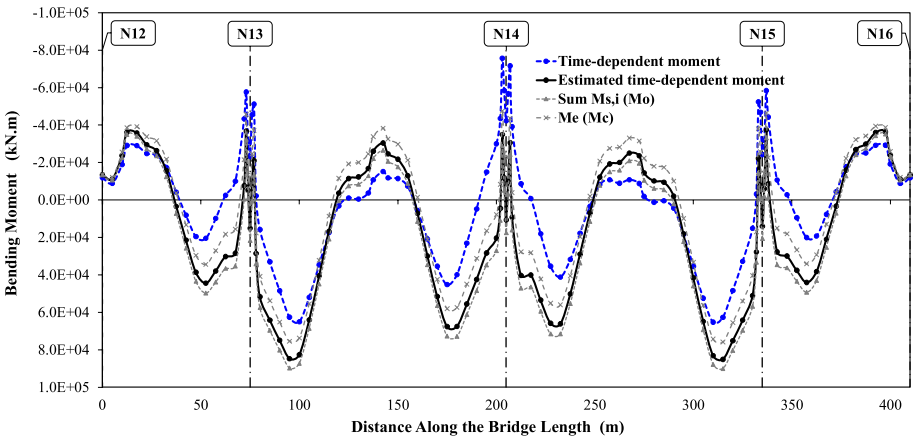

Fig. 16 Time-dependent moments for Girga Bridge from 'real' time history FE analysis versus estimated time-dependent moments from simplified approach

come in line with those presented for El-Warrak Bridge despite differences in concrete dimensions, boundary conditions, prestressing arrangement, etc. between Girga and El-Warrak bridges. As it is clear from Fig. 16, there are again some remarkable variations in the results recuperated from the simplified (through combining time-*independent* results) versus the sophisticated (via real time-*dependent*) analysis approaches.

Case study bridge 3: Talkha Bridge

Talkha Bridge is constructed across Damietta branch of the Nile River to connect the north and south parts of the Nile at Talkha City which is located in the Delta of Egypt. The final bridge structure consists of three continuous spans, i.e., two side spans and one main (navigation) span as shown in Fig. 17. Each side span is 65.0 m long, and the main span is 100.0 m long. The bridge hosts four lanes, two lanes for each traffic direction. The superstructure consists of two parallel identical box girders which are completely

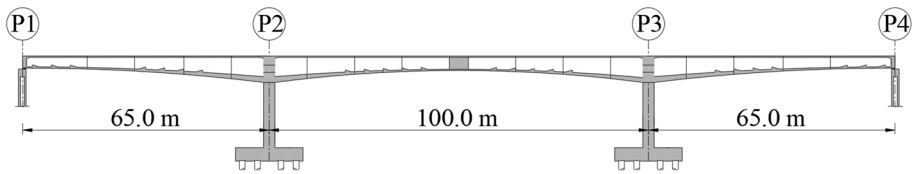

Fig. 17 Elevation of Talkha Bridge over the Nile River

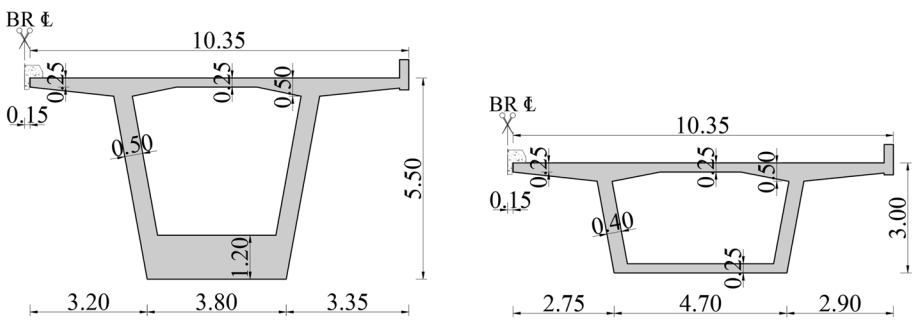

Fig. 18 Typical cross-sections of Talkha Bridge at inner piers and at mid navigation span

separated along the longitudinal direction of the bridge. The cross-sections of the box girder at mid navigation span and at piers are shown in Fig. 18. The width of the top slab is 10.5 m, while the width of the bottom slab varies from 4.70 m at the mid-span to 3.80 m at the piers. The height of the cross-section varies parabolically from 3.0 m at mid-span to 5.50 m at the piers. The bridge deck is supported on longitudinally sliding bearings at edge piers while it is cast integrally with intermediate piers. The longitudinal prestressing layout is shown in Fig. 19. Each prestressing tendon consists of 12 strands. The strand is a 15.2-mm diameter 7-wire low relaxation type. The number of top "cantilever" tendons is 38 around each pier, while the number of bottom "continuity tendons is 18 in the main span and 14 in each side span. The tendons are initially stressed to 75% of the ultimate tensile strength (UTS).

Actual construction sequence

The bridge is incrementally constructed as a balanced cantilever from piers P2 and P3 such that two parts with equal weight can be constructed at the same time around each pier. A total of four cast-in-place segments are located at each side of the two piers P2 and P3. Each segment is cast utilizing conventional formwork in 30 days, while the construction of each pier takes 90 days. After constructing each segment, sufficient tendons are tensioned in the top slab (known as 'cantilever' prestressing) to carry its own weight, and then the formwork is removed. At the two sides of the river, a 17.0-m-long stretch at the end of each side span is cast on temporary scaffolding and is hence connected to the near end of the double cantilevers extending from piers P2 and P3. After the integrated side span hardens, 6 bottom tendons are tensioned in each. The construction of each side span takes 30 days. On the other hand, the tips of the cantilevers in the navigation span are then connected by a 5.0 m closure segment. After the closure segment hardens, 18 bottom 'continuity' tendons are prestressed in the navigation span, along with 8 more bottom tendons in each of the two side spans. The construction of the entire bridge takes 255 days. After all bottom tendons are prestressed, the structure achieves a continuous form and is ready to accept any superimposed load including asphaltic wearing surface and safety barriers, traffic, and other live loads expected on the completed bridge Fig. 20 shows the three-dimensional model of the bridge built to simulate the behavior during construction and throughout the bridge full service life accounting for the long-term time-dependent creep effects.

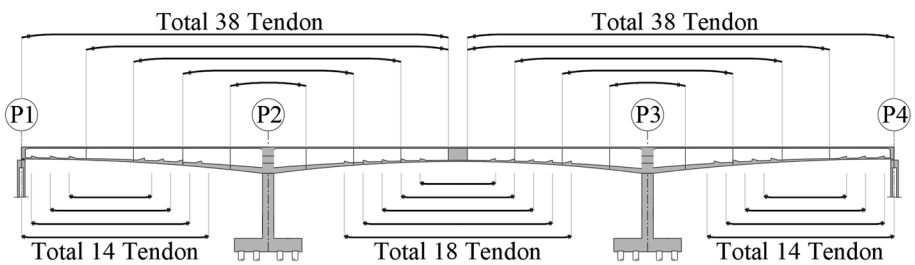

Fig. 19 Longitudinal prestressing layout of Talkha Bridge

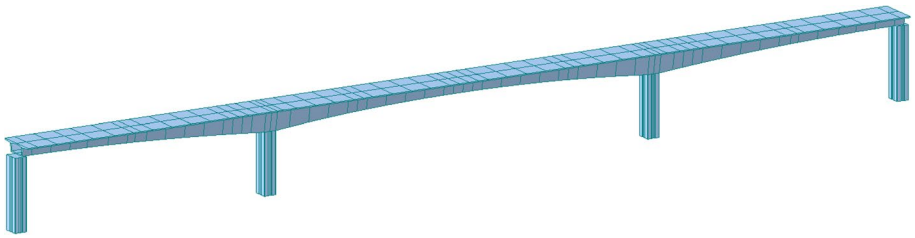

Fig. 20 3D FE model of Talkha Bridge in Midas Civil software

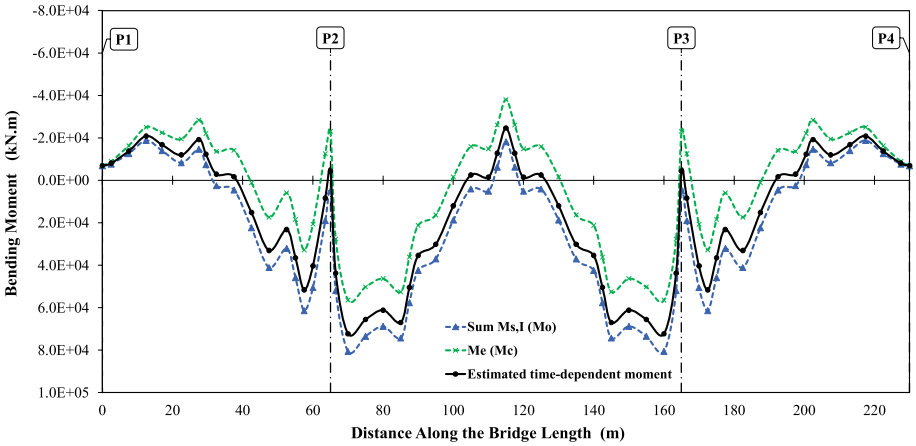

Fig. 21 Estimated time-dependent moments using the simplified approach per Kwak and Son (2002)–Talkha Bridge

Results and comparative assessment

Being majorly different in various aspects from previously analyzed El-Warrak and Girga (quite comparable) bridges, Talkha Bridge has been deliberately selected by the authors to serve as a third case-study to scrutinize earlier observations made on results obtained for the former two bridges. Talkha Bridge has the following distinctive characteristics when compared to both El-Warrak and Girga bridges, namely: (a) it consists of three instead of four spans with only one main (navigation) span; (b) it has different construction conditions and sequence, where each segment is constructed on a movable scaffolding system mounted on removable steel piles which made it possible to use segments with longer length (viz. 12.5 m) relative to the typical cast-in-situ segments of about 5.0 m commonly adopted in balanced cantilever construction; and (c) it features different amount and arrangement of prestressing along the bridge length dependent on its unique segments' length. Results of the simplified approach according to Eq. (2) are shown in Fig. 21 in the form of the estimated final time-dependent moment, M_T, as well as its constituents (namely, $\Sigma Ms,i$ and M_E) resulting from the two simplified time-*independent* FE analyses. Reference could be made to Rashed [30] for relevant creep factors for each segment along the bridge length. On the other hand, the second more precise approach (conducting a real time-dependent analysis) is also accomplished through a sophisticated time history FE analysis using Midas Civil based on actual construction

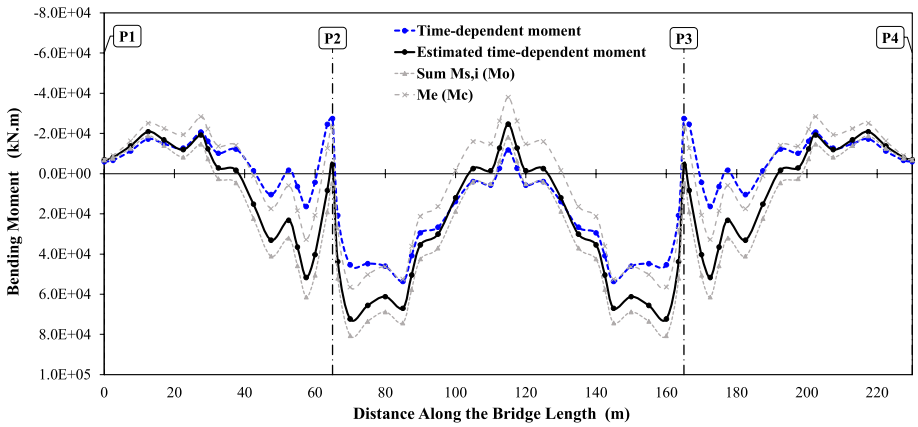

Fig. 22 Time-dependent moments from 'real' time history FE analysis versus estimated time-dependent moment from simplified approach–Talkha Bridge

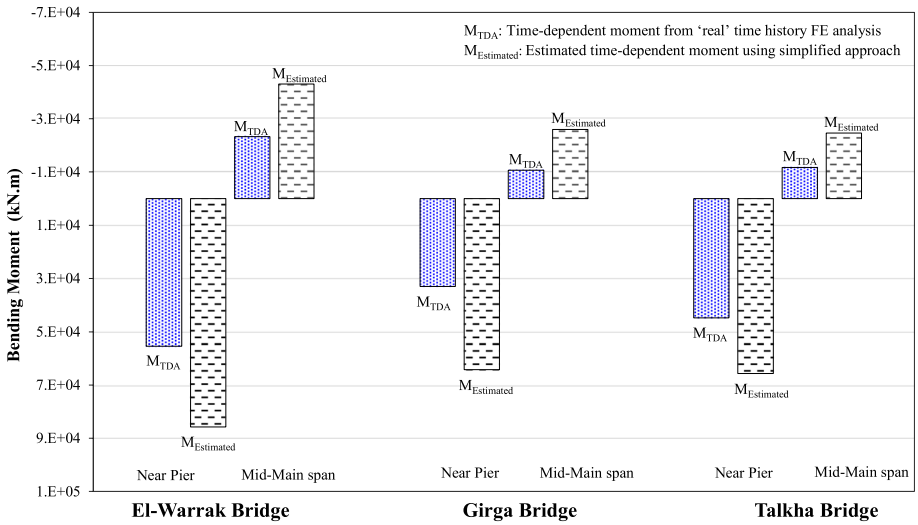

Fig. 23 Comparison of creep-induced permanent loads' bending moments at selected key critical sections from the two design approaches for the three studied bridges (in absence of superimposed dead load and live load effects)

sequence as well as relevant time-dependent parameters. Final time-dependent design moments along the bridge after 10,000 days from end of construction are accordingly computed. Figure 22 illustrates the design time-dependent bending moments along the bridge length according to the two approaches. Despite the prime differences between the characteristics of Talkha Bridge and those of El-Warrak and Girga bridges, results of the three case-study bridges are still fairly alike. Accordingly, one could ascertain that simplified analysis approaches commonly adopted in the literature through combining results from time-independent analyses would definitely lead to considerable and serious errors in estimating design time-dependent moments in bridges constructed using the balanced cantilever technique.

For a useful visualization of the results, a final quantitative comparison of main values of the *time-dependent* bending moments due to permanent loads at selected key critical sections for the three studied bridges according to the two (*simplified* versus *sophisticated*) design approaches adopted herein is illustrated in Fig. 23. It may be clear from results presented that by adding the bending moments from superimposed dead loads and live loads acting on the final completed bridge system, the expected design "total" sagging moment near mid span and the design "total" hogging moment near pier would be on the un-conservative side if the creep-induced permanent loads' moments (referring to Fig. 23) are computed based on the *simplified* time-dependent analysis approach.

Conclusions

The primary focus of this research is to assess the validity and reliability of ad-hoc approaches readily available in the literature and commonly used by the design community for the analysis of prestressed concrete segmental bridges constructed by the balanced cantilever technique. Such approaches have evolved over the years relying on simplified analyses/formulae to cater for time-dependent creep effects on the moment redistribution along the bridge length in light of the lack—until very recently—of specialized commercial analysis software packages able to conduct rigorous and robust actual step-by-step time-dependent analyses. To provide realistic conclusions, three distinct case-study real-world segmental balanced cantilever bridges over the Nile River in Egypt are elected. Relying on critical and comparative review of the results captured by both (a) simplified analyses/formulae and (b) real time-dependent time history analysis, some valuable observations have been pinpointed as in the body of the paper, and the following key conclusions have been drawn:

1. Simplified formulae commonly validated and endorsed by several researchers and designers for creep-induced moment redistribution in typical segmentally constructed RC bridges or prestressed concrete bridges constructed by the span-by-span erection methods may lead to considerable errors if instead applied to estimate the design time-dependent long-term moments in *balanced cantilever* bridges.
2. Unexpectedly to the design community, the final design moment including creep due to self-weight and prestressing long-term effects at all cross-sections along the whole length of a prestressed bridge constructed by the balanced cantilever technique lies outside the range of values bounded by the two time-*independent* moment terms referred to in the simplified formulae readily available in the literature.
3. The exceptionally large amount of top (i.e., cantilever) prestressing typically used in the balanced cantilever segmental bridges to carry the segments' own weight in the 'open', i.e., during construction, configuration generally restricts creep movement produced by sustained self-weight stresses in the 'closed' bridge structural system. Accordingly, the prestressing-induced creep increases the design hogging (i.e., over support) moment magnitude in contradiction with traditional simplified formulae. This actual behavior (and the subsequent rise in the hogging moment) could never be captured by the explicit linear combination format of these formulae since as mathematically anticipated, such equation form shall reveal an estimated final design

time-*dependent* moment along the bridge length always bounded by the two time-*independent* moment terms linearly combined through combination coefficients constrained to a unit sum.

4. The sagging (or generally speaking, 'all within span') time-dependent bending moments precisely accounting for creep due to self-weight and prestressing long-term effects through real time history analysis are appreciably reduced relative to their counterpart values estimated through the linear combination simplified formulae available in the literature.

Further investigations involving other real-world prestressed concrete bridges constructed using the balanced cantilever techniques and featuring different span configurations, cross-section properties, amount and arrangement of prestressing cantilever and/or continuity tendons, construction duration, etc. shall be performed in order to decide whether the above conclusions shall be retained or further refined.

Abbreviations

M_T	Estimated time-dependent moment
M_E, M_C	Moment obtained by assuming the entire structure constructed at the same stage
ΣMs,i, $\Sigma M_{O\,j}$	Combined elastic moments that occur at successive construction steps
φ	Creep coefficient
ρ	Relaxation factor
χ	Concrete ageing coefficient
α	Contribution of $\Sigma M_{s,i}$ in estimating time-dependent moment
β	Contribution of ΣM_E in estimating time-dependent moment
t_o	Age of segment at loading
t_1	Age at segment placement
t_2	10,000 Days (long term)
h_o	Notional size of the member (segment)
φ_o	Notional creep coefficient
φ_{RH}	Factor to allow for the effect of relative humidity on the notional creep coefficient
$\beta(t_o)$	Factor to allow for the effect of concrete age at loading on the notional creep coefficient
β_H	Coefficient depending on the relative humidity
$\beta c(t,t_0)$	Coefficient to describe the development of creep with time after loading

Acknowledgements
The authors are very grateful to Dr. Samer Youakim of Dar Al-Handasah Bridge Department, Cairo, Egypt, for the valuable discussions and for his fruitful comments throughout the research.

Authors' contributions
MR collected the data, created the analysis models using Midas Civil, analyzed the results, and wrote the paper. SM guided, supervised, evaluated the results, and assisted MR in writing the paper. All authors read and approved the final manuscript.

Funding
The authors declare that they did not receive any funding sources.

Availability of data and materials
The datasets used and/or analyzed during the current study are available from the corresponding author on reasonable request.

Declarations

Competing interests
The authors declare that they have no competing interests.

Received: 31 January 2023 Accepted: 6 April 2023
Published online: 18 April 2023

References

1. Gabaldón LBF, Pérez JFR, Paredes JK (2020) Moment redistribution in segmental Cantilever Bridges: simplified approach. Pract Period Struct Des Constr 25(3):06020005. https://doi.org/10.1061/(ASCE)SC.1943-5576.0000486

2. Zejak D (2015) Approximate methods for analysing the effects of creeping and shrinkage of reinforced and prestressed concrete constructions. Procedia Eng 117(2015):712–722. https://doi.org/10.1016/j.proeng.2015.08.199
3. Bazant ZP, Qiang Y, Li G (2012) Excessive long-time deflections of prestressed box girders. I: Record-span bridge in Palau and other paradigms. J Struct Eng 138(6):676–686. https://doi.org/10.1061/(ASCE)ST.1943-541X.0000487
4. Bazant ZP, Qiang Y, Li G (2012) Excessive long-time deflections of prestressed box girders. II: Numerical analysis and lessons learned. J Struct Eng 138(6):687–696. https://doi.org/10.1061/(ASCE)ST.1943-541X.0000375
5. Ates S (2011) Numerical modelling of continuous concrete box girder bridges considering construction stages. Appl Math Model 35(8):3809–3820. https://doi.org/10.1016/j.apm.2011.02.016
6. Bazant ZP, Hubler MH, Yu Q (2011) Excessive creep deflection: an awakening. Concr Int 33(8):44–46
7. Yu Q, Bazant ZP, Wendner R (2012) Improved algorithm for efficient and realistic creep analysis of large creep-sensitive concrete structures. ACI Struct J 109(5):665–675
8. Chiorino MA (2005) A rational approach to the analysis of creep structural effects. In: Gardner NJ, Weiss W (eds) Shrinkage and creep of concrete. American Concrete Institute (ACI), Farmington Hills, pp 107–141
9. Kwak H-G, Seo Y-J (2000) Long-term behavior of composite girder bridges. Comput Struct 74:583–599. https://doi.org/10.1016/S0045-7949(99)00064-4
10. Bazant ZP, Baweja S (2000) Creep and shrinkage prediction model for analysis and design of concrete structures: model B3. In: Al-Manaseer A (ed) Proc., Adam Neville Symp.: creep and shrinkage-structural design effects. American Concrete Institute (ACI), Farmington Hills, pp 1–83
11. Bishara AG, Papakonstantinou NG (1990) Analysis of cast-in-place concrete segmental cantilever bridges. J Struct Eng 116(5):1247–1268. https://doi.org/10.1061/(ASCE)0733-9445(1990)116:5(1247). ASCE
12. Chiu HI, Chern JC, Chang KC (1996) Long-term deflection control in cantilever prestressed concrete bridges I: Control method. J Eng Mech 12(6):489–494. https://doi.org/10.1061/(ASCE)0733-9399(1996)122:6(489). ASCE
13. Ketchum MA (1986) Redistribution of stresses in segmentally erected prestressed concrete bridges, UCB/SESM-86/07. Department of Civil Engineering, University of California, Berkeley
14. Trost H, Wolff HJ (1982) Zur wirklichkeitsnahen ermittlung der beanspruchungen in abschnittswiese hergestellten spannbetonragwerken. Structural Engineering Documents 1e, Concrete Box-Girder Bridge, IABSE
15. Cruz PJS, Mari AR, Roca P (1998) Nonlinear time-dependent analysis of segmentally constructed structures. J Struct Eng 124(3):278–288. https://doi.org/10.1061/(ASCE)0733-9445(1998)124:3(278). ASCE
16. Barker JM (1997) Post-tensioned box girder manual. Post-Tensioning Institute, USA
17. Kwak H-G, Son J-K (2002) Determination of design moments in bridges constructed by balanced cantilever method. Eng Struct 24(5):639–648. https://doi.org/10.1016/S0141-0296(01)00128-6
18. Kwak H-G, Seo Y-J, Jung C-M (2000) Effects of the slab casting sequences and the drying shrinkage of concrete slabs on the short-term and long-term behavior of composite steel box girder bridges. Part I. Eng Struct 23:1453–1466. https://doi.org/10.1016/S0141-0296(99)00095-4
19. Kwak H-G, Seo Y-J, Jung C-M (2000) Effects of the slab casting sequences and the drying shrinkage of concrete slabs on the short-term and long-term behavior of composite steel box girder bridges. Part II. Eng Struct 23:1467–1480. https://doi.org/10.1016/S0141-0296(99)00096-6
20. ACI Committee 209 (1970) Prediction of creep, shrinkage and temperature effects in concrete structure. In: Paper SP 27–3 in ACI Special Publications SP-27, Designing for effects of creep, shrinkage, temperature in concrete structures
21. Neville AM, Dilger WH, Brooks JJ (1983) Creep of plain and structural concrete. Construction Press, London. https://catalogue.nla.gov.au/Record/1817421
22. Bazant ZP (1972) Prediction of concrete creep effects using age-adjusted effective modulus method. ACI J 69(4):212–217
23. Gendy A, Rashed M (2018) Simplified computation of time dependent effects of segmental bridges. Int J Bridge Eng 6(2):85–107. https://www.ijbe.net/issues/volumes/item/download/274_fdb9c9589cc2b0eafa8496e32a552290
24. Pimanmas A (2007) The effect of long-term creep and prestressing on moment redistribution of balanced cantilever cast-in-place segmental bridge. Songklanakarin J Sci Technol 29(1):33–39. https://doaj.org/article/dea2093d579b4119ab1977c92bc283e5
25. Schlaich J, Scheef H (1982) Concrete box-girder bridges. Structural Engineering Documents 1e, Concrete Box-Girder Bridge, IABSE
26. EN 1992-1-1 Eurocode 2 (2004) Design of concrete structures. Part 1-1: general rules and rules for buildings. Comité Européen de Normalisation, Brussels
27. EN 1992-2 Eurocode 2 (2005) Design of concrete structures. Part 2: concrete bridges – design and detailing rules. Comité Européen de Normalisation, Brussels
28. CEB-fib (2013) fib model code for concrete structures 2010. Wiley, Netherlands, ISBN: 978-3-433-60408-3
29. AASHTO LRFD (2020) AASHTO LRFD bridge design specifications, 9th Ed., American Association of State Highway and Transportation Officials, Washington
30. Rashed M (2022) Determination of design time-dependent moments for prestressed concrete balanced cantilever bridges - known simplified approach VS actual time-dependent analysis. PhD. Thesis, Structural Engineering Dept., Cairo University, Giza

Publisher's Note